ACS APPLIED MATERIALS & INTERFACES

Research Article

www.acsami.org

Hydroxyapatite Formation on Sol–Gel Derived Poly(ε-Caprolactone)/Bioactive Glass Hybrid Biomaterials

Bedilu A. Allo,[†] Amin S. Rizkalla,*[,†,‡] and Kibret Mequanint*[,†]

[†]Department of Chemical and Biochemical Engineering, The University of Western Ontario, London, ON, Canada N6A 5B9

[‡]Biomaterials Science, Schulich School of Medicine and Dentistry, The University of Western Ontario, London, ON, Canada N6A 5C1

Supporting Information

ABSTRACT: Investigation of novel biomaterials for bone regeneration is based on the development of scaffolds that exhibit bone-bonding ability, biocompatibility, and sufficient mechanical strength. In this study, using novel poly (ε-caprolactone)/bioactive glass (PCL/BG) hybrids with different organic/inorganic ratios, the effects of BG contents on the in vitro bone-like hydroxyapatite (HA) formation, mechanical properties, and biocompatibility were investigated. Rapid precipitation of HA on the PCL/BG hybrid surfaces were observed after incubating in simulated body fluid (SBF) for only 6 h, as confirmed by scanning electron microscopy (SEM), energy dispersive X-ray spectroscopy (EDX), Fourier-transform infrared spectroscopy (FTIR), and inductively coupled plasma atomic emission spectroscopy (ICPS). The ICPS elemental analysis results were further analyzed in terms of the Ca^{2+} and PO_4^{3-} which were consumed to form the apatite layer. The results revealed that the rate and total amount of HA deposition decreased with an increase in PCL content. The compressive modulus and strength of the PCL/BG hybrids increased with the decrease in PCL content. The highest values were achieved at the lowest PCL content (10 wt %) and were around, 90 MPa and 1.4 GPa, respectively. To evaluate the cytotoxicity of PCL/BG bioactive hybrids, MC3T3-E1 osteoblast-like cells were cultured for up to 72 h. Our data indicated that whereas initial cell attachment was marginally lower than the control tissue culture poly styrene (TCPS) surface, the hybrid materials promoted cell growth in a time-dependent manner. Cell viability within the different PCL/BG hybrid samples appeared to be influenced by compositional differences whereby higher PCL contents correlated with slight reduction in cell viability. Taken together, this study adds important new information to our knowledge on hydroxyapatite formation, mechanical properties, and cytotoxic effects of PCL/BG hybrids prepared by the sol–gel process using a tertiary glass composition and may have considerable potential for bone tissue regeneration applications.

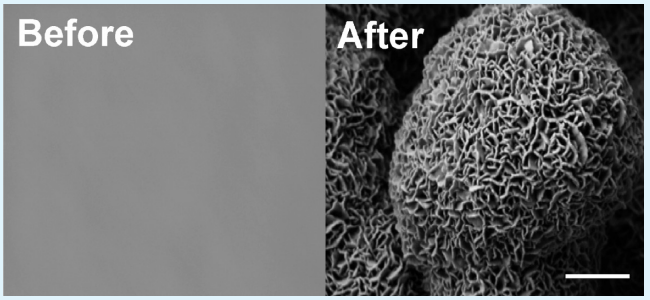

KEYWORDS: *bone regeneration, organic–inorganic hybrids, poly (ε-caprolactone), bioactive glass, bioactivity*

INTRODUCTION

Development of novel biomaterials represents an essential area of interest in bone tissue engineering strategies.[1] A variety of biomaterials, including natural and synthetic polymers and ceramics,[2] are being used to fabricate synthetic scaffolds which act as guides and stimuli for tissue regeneration.[3] In general, scaffolds for bone tissue regeneration are required to be, at the very least, capable of supporting cell attachment, and provide sufficient mechanical strength, bioactivity, and biodegradability.[4] For this reason, bioactive glasses (BG) and biodegradable synthetic polymers were among the most widely studied materials for bone tissue engineering.[5,6] BG-based biomaterials are known for their biocompatibility, osteoinductivity, osteoconductivity, and ability to form a bone-like mineral phase at the interface when in contact with living tissues.[7,8] However, BGs are stiff and brittle, making them difficult to be formed into complex shapes, and are susceptible to fracture under mechanical loads.[9] Although aliphatic polyesters such as poly (glycolic acid) (PGA), poly (L-lactic acid) (PLA), poly (ε-caprolactone) (PCL), and their copolymers have been extensively investigated as potential scaffold materials for bone tissue engineering,[10] they have shown limited strength and mechanical stability to match with bone tissue, especially when fabricated with large volume fractions of macroporosity.[11] In addition, they are not osteoconductive and do not directly bond to bone. Despite the availability of different materials, it has been a challenge to find a single material that is both mechanically competent and biodegradable. Recently, sol–gel derived organic–inorganic (O/I) hybrid material from biodegradable polymers and bioactive inorganic materials have been developed with the aim of increasing mechanical stability and improving tissue interaction during bone regeneration.[12−14] O/I hybrid biomaterials are based on selective combination of either biostable[15,16] or biodegrad-

Received: March 19, 2012
Accepted: May 25, 2012
Published: May 25, 2012

   dx.doi.org/10.1021/am300487c | ACS Appl. Mater. Interfaces 2012, 4, 3148–3156

able[12,17] polymers and bioactive glasses which are expected to exhibit tailored physical, biological, and mechanical properties. In addition, this type of structural organization of synthetic materials resembles the structure of bone tissue, where the inorganic component mimics the hydroxyapatite and the polymer component mimics the collagen-rich extracellular matrix.[18]

The requirement for the O/I hybrids to bond to living bone is the formation of a biologically active hydroxyapatite (HA) layer on their surface when they are exposed to physiological fluid. The in vitro bone-like HA layer formation ability of bone-forming biomaterials, evaluated in a simulated body fluid (SBF),[19] is generally thought to facilitate recruitment of proteins such as collagen, fibronectin, and vitronectin, in which osteoblasts bind and proliferate,[20] thereby allowing for the formation of an intimate bond to bone. The modification of the inorganic network by adding organic polymers in the O/I hybrid materials were suggested to influence the bioactivity and the mechanical properties of the resultant hybrid materials.[15,21] For example, in the PCL/silica hybrid system, higher PCL content showed a lower apatite-forming rate and polymer-like ductile−tough fracture behavior than lower PCL content which showed a higher rate of apatite formation and ceramic-like hard−brittle fracture behavior.[2215] Results from these studies imply that, by varying the polymer to inorganic (i.e., Silica) ratio, the bioactivity and mechanical properties of the hybrid material could be tailored. Other studies also showed that incorporation of Ca^{2+} in the hybrid system provided an improved osteoconductivity and in vitro bone-like apatite formation ability of the hybrid system.[23] Another aspect of vital importance in preparing a scaffold material for bone regeneration is biocompatibility of the scaffold material to the host tissue. Sol−gel derived bioactive and biodegradable O/I materials are presumed to be cytocompatible only after calcination (ca. 600 °C) and removal of the polymer template used for the sol−gel process.[24−28] Obviously, once the polymer is degraded, the materials are no longer O/I hybrids. Sol−gel derived O/I hybrid materials are prepared at low temperature to facilitate silicate hydrolysis and avoid phase separation between the organic and inorganic components. In the absence of high temperature treatment that removes unreacted species and/or traces of trapped impurities, the sol−gel approach could be a major source of concern to the cytocompatibility of this class of biomaterials. Although data is scanty, cellular responses to sol−gel derived O/I hybrids without high-temperature treatment generally showed poor results[23] even with attempts to neutralize the residual HCl that may be present in the samples.[29]

Notwithstanding the above reports, systematic data on O/I hybrid materials with biodegradable polymer and tertiary glass components is notably lacking. Previously, we have reported the synthesis and characterization of bioactive and biodegradable PCL/BG hybrid biomaterials with different organic to inorganic ratios via a sol−gel process.[12] In that study, we have also demonstrated a PCL/BG hybrid scaffold fabrication by the electrospinning process.[12] However, the suitability of these novel hybrid biomaterials for potential bone tissue engineering applications was not studied. Therefore, the objective of the present study was to investigate the effect of composition on the in vitro bone-like apatite formation ability, mechanical property, and cytotoxicity of the PCL/BG hybrid biomaterials synthesized via a sol−gel process. This study adds important new information to our knowledge of rapid hydroxyapatite formation on PCL/BG surfaces prepared by the sol−gel process using a biodegradable polymer and a tertiary glass composition.

EXPERIMENTAL SECTION

Preparation of PCL/BG Hybrid Materials. PCL/BG hybrids were synthesized via a sol−gel process as described previously.[12] Briefly, a known amount of PCL (CAPATM 6800, MW 80 000 g/mol) pellets were dissolved in methyl ethyl ketone (MEK) at 35 °C under moderate stirring for 12 h. After the PCL is completely dissolved, tetraethyl orthosilicate (TEOS), DI water, triethyl phosphate (TEP), and $CaCl_2{\cdot}2H_2O$ were added successively under vigorous stirring in the presence of a catalytic amount of 1N HCl. Hydrolysis of TEOS was carried out at 35 °C until a homogeneous and transparent sol was obtained. Following this, the sol was sealed and kept in an oven at 50 °C for 72 h. Aging and drying of PCL/BG hybrid gels were carried out at 60 °C for 7 days. The compositions of PCL/BG hybrids used in this study are summarized in Table 1.[12]

Table 1. Compositions of PCL/BG Hybrid Biomaterials

PCL/BG (wt %)	sample code
0/100	BG
10/90	1090
40/60	4060
60/40	6040
100/0	PCL

In Vitro Bioactivity of PCL/BG Hybrids. The in vitro bioactivity of the PCL/BG hybrid and control PCL disk samples (6 mm × 2 mm) were carried out by incubating in SBF.[19] The SBF solution has a composition and concentration similar to those of the inorganic part of human plasma (see Table S1 in the Supporting Information). One liter of SBF solution was prepared by dissolving NaCl (7.996 g), $NaHCO_3$ (0.350 g), KCl (0.224 g), $K_2HPO_4{\cdot}3H_2O$ (0.228 g), $MgCl_2{\cdot}6H_2O$ (0.305 g), $CaCl_2$ (0.278 g), and Na_2SO_4 (0.071 g) into distilled water and buffering at pH 7.4 with tris (hydroxymethyl) amminomethane $(HOCH_2)_3CNH_2$ (6.057 g) and an appropriate amount of 1N HCl. The as-prepared PCL/BG hybrid monoliths were pulverized by a ball mill for 5 min; then 0.05 g of powder was weighed and heat pressed using a custom-made stainless steel mold to prepare PCL/BG hybrid disks with an approximate dimension of 6 mm in diameter and 2 mm in thickness. Each specimen was immersed in 20 mL of SBF (0.05 g/20 mL) contained in polypropylene bottles covered with a tight lid. The bottles were placed in an orbital shaker at a constant speed of 120 rpm and temperature of 37 °C from 6 to 168 h without SBF refreshing. After each soaking period, the disks were collected from the SBF and rinsed thoroughly with phosphate-buffer saline (PBS) and ethanol and dried overnight at 37 °C.

Scanning Electron Microscopy and Energy Dispersive X-ray Spectroscopy. The morphology of HA-like crystals precipitated on the disks surface during the incubation period was observed using a high resolution scanning electron microscopy (Leo 1540 FIB/SEM with Cross-Beam, 25 kV, Zeiss Nano Technology Systems Division, Germany). The growth and elemental composition of the HA-layer formation were also evaluated by using an energy dispersive X-ray spectroscopy (EDX) detector attached to the S-2600N SEM. All disks were coated with 3 nm of osmium using a Filgen OPC-80T osmium plasma coater prior to SEM imaging.

Inductively Coupled Plasma Spectroscopy. The concentrations of calcium, phosphate, and silicon ions in the SBF solution during the incubation period were determined using the inductively coupled plasma optical-emission spectroscopy (ICP-OES; Vista-Pro Axial, Varian Inc., USA). Furthermore, Ca^{2+} and PO_4^{3-} ion consumption in SBF to form the HA layer were calculated as follows:

$$X_{\text{consumption}} = X_{\text{max in SBF}} - X_{\text{final in SBF}}$$

where X indicates either Ca^{2+} or PO_4^{3-} ion concentrations and $X_{max\ in\ SBF}$ and $X_{final\ in\ SBF}$ were determined from the time-course inductively coupled plasma atomic emission spectroscopy (ICPS) measurements.

Fourier Transform Infrared Spectroscopy. The Fourier transform infrared spectroscopy (FTIR) absorption spectra were collected using the Bruker IFS 55 FTIR (Bruker Optics, Billerica, MA). After soaking in SBF, the specimens were powdered, and 2 mg of each sample was mixed with 200 mg of potassium bromide (KBr) powder, pressed as a pellet, and scanned at a resolution of 4 cm^{-1} and sample scans of 32. All spectra were analyzed utilizing the OPUS software version 4.0. Identification of the absorption bands was based on previous study on synthetic and biological apatite.[30]

X-ray Diffraction. XRD measurements of the samples were carried out using a rotating anode X-ray diffractometer model RTP300 (Rigaku Rotaflex, Japan) operating on Co Kα radiation and run at 45 kV and 160 mA. Samples for XRD measurements were prepared by crushing the PCL/BG hybrid disks before and after incubating in SBF. XRD measurements were conducted in the 2θ range from 2 to 82° with step size of 0.02. Two 2θ for equivalent Cu Kα radiation was obtained using Bragg's law, $\lambda = 2d \sin\theta$ and $\theta_{Cu} = \sin^{-1}(\lambda_{Cu}\sin\theta_{Co}/\lambda_{Co})$, where, λ_{Cu} = 1.54056 Å and λ_{Co} = 1.79026 Å.

Compressive Testing. PCL/BG hybrid and the PCL control cylindrical specimens (n = 5) with 3:2 aspect ratio (9 mm in height and 6 mm in diameter) were used for compressive mechanical testing. An uniaxial compression test was conducted using an Instron Universal Mechanical testing machine equipped with 5 kN load cell (Instron model 3345, Canton, MA) with crosshead speed of 1 mm/min at ambient temperature and humidity. The compressive modulus was determined from the slope of the initial linear elastic portion of the stress−strain curve. The maximum strength of the PCL/BG hybrid specimens were also determined using the software associated with the Instron machine.

Cytotoxicity Assay. For colorimetric assay of the metabolic activity of viable cells, nonradioactive Cell Proliferation Kit I (MTT; Roche, Toronto, ON, Canada) was used. In this technique, the yellow tetrazolium salt (3-(4,5-dimethylthiazol-2-yl)-2,5-diphenyltetrazolium bromide (MTT)) is reduced to a purple formazan compound by the dehydrogenase activity of intact mitochondria. Consequently, this conversion only occurs in living cells. For the purpose of this assay, the PCL/BG hybrid powders were first sterilized using ultraviolet (UV) light for 1 h. Following this, a known amount of PCL/BG hybrid powders were dispersed in serum-free culture media (α-MEM) using ultrasonic irradiation for 20 min to make up 2 mg/L suspension. MC3T3-E1 osteoblast-like cells (generously provided by Dr. Jeff Dixon at the University of Western Ontario) were seeded in 96-well tissue culture plates at an initial density of 1×10^4 cells per well. A final volume of 100 μL of cultured medium per well containing α-MEM supplemented with 10% FBS and 100 U/mL of penicillin and 100 μg/mL of streptomycin were used. Cultures were incubated for 24 h in a humidified atmosphere of 95% air and 5% CO_2, at 37 °C. The PCL/BG hybrid suspension at concentrations of 100, 200, 300, and 500 μg/mL was then added in the confluent layer of MC3T3-E1 osteoblast-like cells. After 24 and 72 h of incubation period, 10 μL of MTT solution (5 mg/mL in PBS) was added to each well followed by incubation in a humidified atmosphere at 37 °C for 4 h. For dissolution of the purple formazan crystals formed after the incubation period, 100 μL of the solubilization solution (10% SDS in 0.01 M HCl) was added and incubated overnight in a humidified atmosphere at 37 °C . The optical density (OD) of each well at the absorbance wavelength of 595 nm was determined by a microplate reader (ELX 800, Bio-Tek, USA) with a reference wavelength of 650 nm. Tissue culture poly styrene (TCPS) was used as a control. The cell-free culture medium with respective PCL/BG hybrid suspension was used as a blank. Triplicates of each sample were tested for each incubation time. The data obtained were then normalized with respect to the OD value of the TCPS at the 6 h culture.

Statistical Analysis. Statistical data analyses were conducted using a one-way analysis of variance (ANOVA) and Tukey HSD Rank Order Test. A probability value of 95% ($p < 0.05$) was used to determine the level of significance. Error is reported in the figures as the standard deviation (SD).

RESULTS

In Vitro Bioactivity of PCL/BG Hybrid Materials. *Scanning Electron Microscopy and Energy Dispersive X-ray Spectroscopy.* The SEM micrographs of the PCL/BG hybrid and PCL disk surface before and after different incubation times in SBF solution are shown in Figure 1. Before incubation

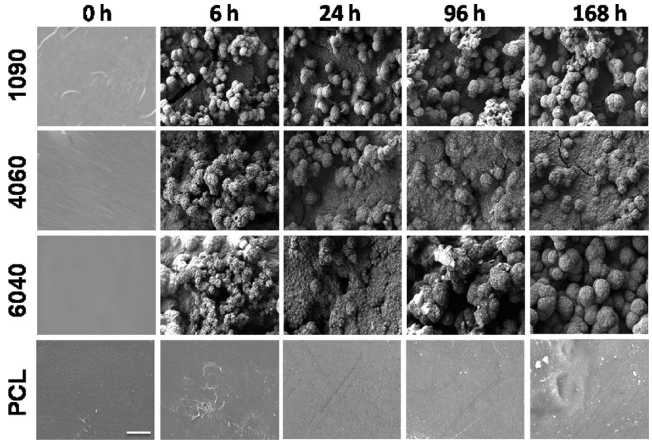

Figure 1. SEM micrographs showing the evolution of the HA layer on different PCL/BG hybrids and PCL control disk surfaces after incubating in SBF at different time points. 0 h represents the samples before incubation starts. (Scale bar = 5 μm.)

in SBF solution (0 h), all the PCL/BG hybrid samples with different compositions showed a smooth surface. After 6 h, the PCL/BG hybrid surfaces were covered with heterogeneous and sparsely dispersed spherically shaped particles. After 24 h of soaking, the surfaces were covered with densely packed particles.

In Figure 2, a high magnification of the micrographs taken for a representative 4060 PCL/BG sample is presented. Similar to typical HA morphology, these micrographs showed evidence of needle-like crystallites covering the PCL/BG hybrid disks. The observed morphology of the HA apatite layer on the surface of PCL/BG hybrid disks was similar for all compositions (see additional micrographs in Figure S1 of the Supporting Information). To the contrary, no apatite layer deposition was observed on the PCL control disks for all time points up to 168 h incubation.

To demonstrate the evolution of apatite layer deposition on the specimen surfaces with respect to the incubation time, the EDX elemental intensities from Figure 2 were converted into wt % and are presented in Figure 3. Before incubation (0 h), the EDX spectrum showed that the surface of the PCL/BG hybrid had large amounts of silicon (65 wt %) compared with the other inorganic constituents (29 wt % Ca and 6 wt % P). After incubation in SBF from 6 to 168 h, the EDX analysis detected an increase in Ca and P concentrations compared with the Si content. Both the increase of Ca and P and the decrease of Si were sharp at the earlier incubation times before it leveled off after 96 h of incubation. The Si content on the surface became extremely low, likely due to the consequence of the thickness of the newly formed apatite layer and the limitation on the X-ray beam penetration depth. The Ca/P ratio after 168 h was calculated to be 1.70 ± 0.04 which is slightly higher than

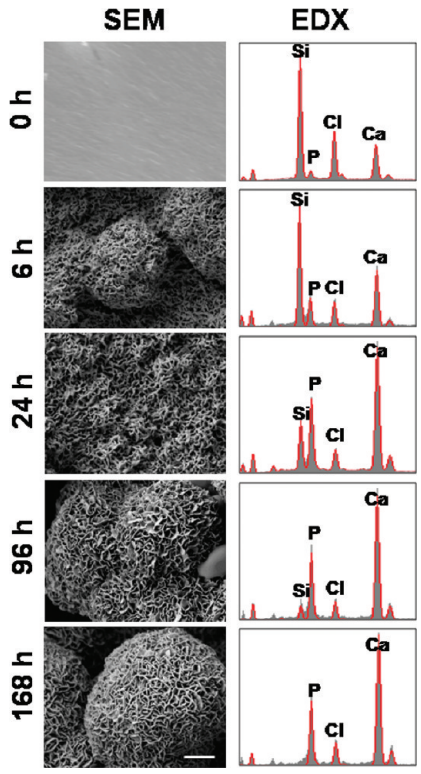

Figure 2. High magnification SEM micrographs and the corresponding EDX patterns for the evolution of the HA layer on 4060 PCL/BG hybrid disks before and after incubation in SBF for different time points. (SEM scale bar = 1 μm.)

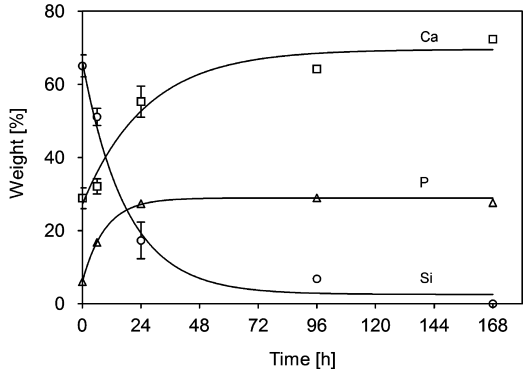

Figure 3. Composition (wt %) profiles of Si, Ca, and P atoms on the surface of 4060 PCL/BG hybrid disks (as determined by EDX) before and after incubation in SBF for different time points.

the stoichiometric ($Ca_{10}(PO_4)_6(OH)_2$) Ca/P ratio (1.67), possibly due to the B-type CO_3^{2-} substitution in apatite lattice.[31] The observation from SEM and EDX studies clearly confirmed that the new surface was enriched by Ca and P, which are the main constituents of HA.

At the 25 keV primary electron beam used in our experiment, the penetration depth at which the primary electrons have sufficient energy to generate characteristic X-rays is limited to about 2−5 μm thick. We therefore measured the apatite layer thickness at different times. To do this, specimen surfaces were scratched to disrupt the deposited HA layer and cross sectional images were taken at 45° angle. The data collectively presented in Figure 4 showed that the film thickness increased significantly from 2 μm at 6 h incubation to 21 μm at 168 h of incubation with SBF.

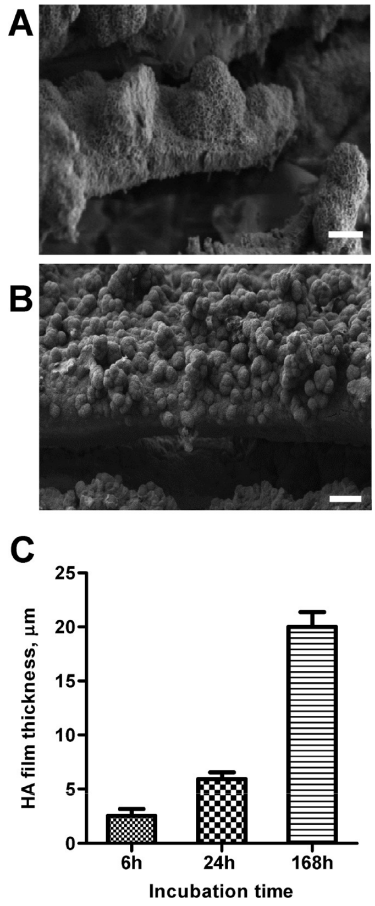

Figure 4. HA film thickness variation with incubation time for 4060 PCL/BG hybrid disks as determined by SEM (A, B) followed quantification using ImageJ (C). Scale bar: A = 2 μm; B = 10 μm.

Inductively Coupled Plasma Spectroscopy. When PCL/BG hybrids are incubated in SBF, the first step is the release of Ca^{2+}, PO_4^{3-}, and Si ions from the PCL/BG hybrid disks into the SBF solution. This is followed by the redeposition (consumption) of the released ions as well as the ions in the SBF solution to the disks to form the HA layers. We therefore measured the concentration variations of these ions in the SBF with the incubation time by means of ICPS. At earlier incubation times, the ions increased sharply in the SBF solution before it decreased due to Ca^{2+} and PO_4^{3-} ions deposited to the hybrid disks (see Figure S2 in the Supporting Information). The consumption of Ca^{2+} and PO_4^{3-} by each sample was calculated by subtracting the final concentration at 96 h from the maximum concentration at 6 h. The data presented in Figure 5 demonstrated that the total consumption for both Ca^{2+} and PO_4^{3-} ions varied with composition. Significantly lower Ca^{2+} and PO_4^{3-} consumption from the SBF solution were observed for 6040 and PCL disks ($p < 0.05$). In the extreme case of the control PCL, a negligible amount of ions were consumed. Furthermore, the results from Figure 5 indicated the amount of CaP deposited on the surfaces of the PCL/BG hybrid samples, which may be used as one of the screening criteria for the evaluation of in vitro bioactivity of materials.

dx.doi.org/10.1021/am300487c | ACS Appl. Mater. Interfaces 2012, 4, 3148−3156

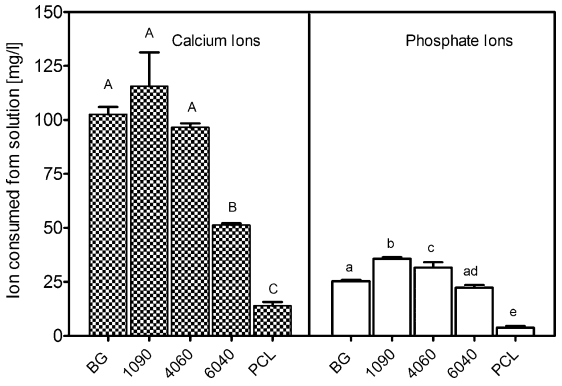

Figure 5. Total consumption of Ca^{2+} and PO_4^{3-} ions from the SBF solution during the in vitro bioactivity test conducted for PCL/BG hybrids with different compositions. Different letters indicate that the groups are significantly different at $p < 0.05$.

Fourier Transform Infrared Spectroscopy. The growth of HA crystals on PCL/BG hybrid sample was also investigated by FTIR spectroscopy before and after incubation for up to 168 h (7 days) in SBF. The IR absorption spectra for PCL/BG hybrid samples and pure BG after various incubation times in SBF are displayed in Figure 6.

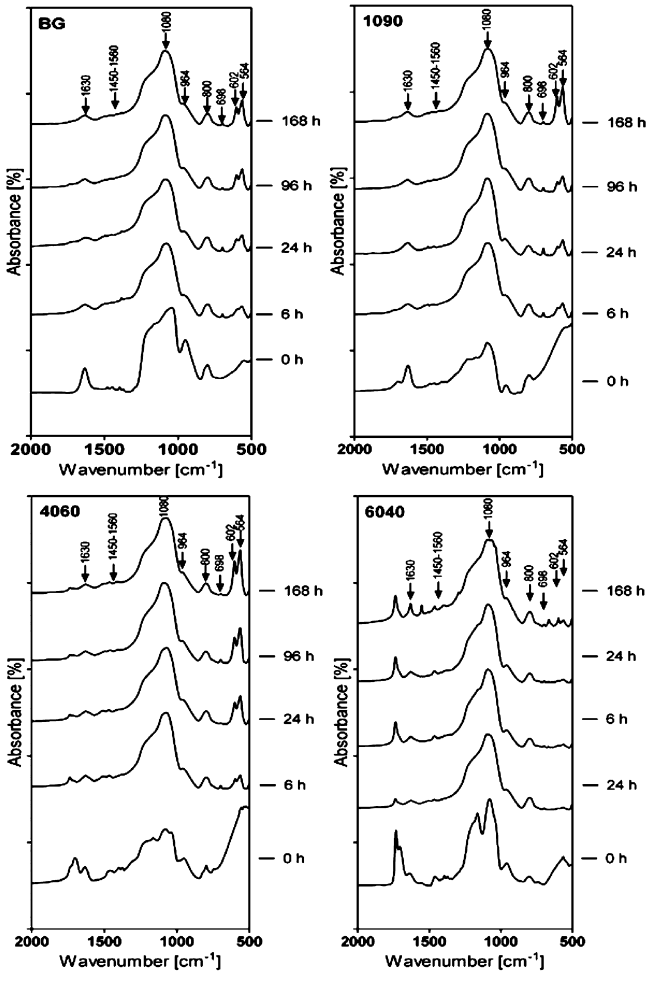

Figure 6. FTIR spectra of the in vitro HA formation on the surface of the PCL/BG hybrid and pure BG disks after incubating in SBF for different time points.

The spectra of the PCL/BG hybrid samples before incubation in SBF showed the absorption peak of the bending and stretching vibrations of Si−O−Si bonds at the wavelength of 800 and 1080 cm^{-1}. The peak at 1630 cm^{-1} is attributed to −OH groups from residual moisture. The characteristic peaks of PCL are observed at 1730 cm^{-1} (C═O). However, after incubation in SBF for 6 h, a weak P−O vibrational band near 602 cm^{-1} was detected, indicating the initial presence of CaP-rich layer. After immersion in SBF for 24 h, two crystalline P−O vibrational peaks at 564 and 602 cm^{-1} were clearly observed. With increased incubation time, the other vibrational peaks of HA were also gradually detected, indicating the evolution of HA as a function of time. The IR spectra of the PCL/BG hybrid samples incubated for more than 96 h showed well-resolved vibrational peaks at 1080 and 800 cm^{-1}, which were assigned to the Si−O−Si bands; the peaks at 1492 cm^{-1} were assigned to the C−O vibration bands; the peaks at 964, 602, and 564 cm^{-1} were assigned to the P−O bands.[30]

X-ray Diffraction. The XRD patterns for PCL/BG hybrid and pure BG samples before and after incubation in SBF up to 168 h are shown in Figure 7. The unincubated BG and PCL/

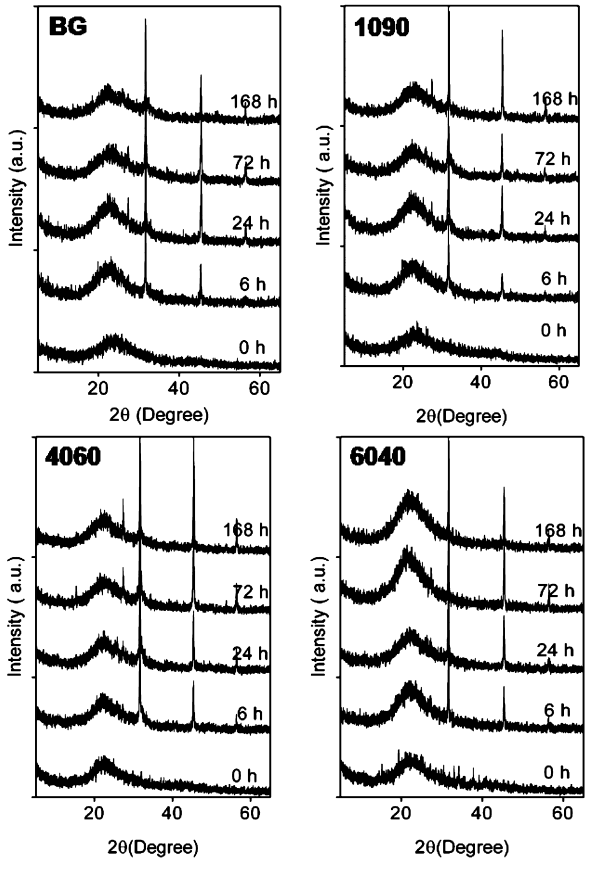

Figure 7. XRD pattern of the in vitro HA formation on the PCL/BG hybrid and pure BG materials surface after soaking in SBF at different time points.

BG hybrid samples (0 h) showed no diffraction peaks indicating that the samples were completely amorphous. In contrast, after 6 h of incubation the apatite diffraction peaks appeared at 2θ = 21.8°, 25.9°, 31.77°, 45.4°, and 53.45°, which were indexed to be (200), (002), (211), (222), and (004) diffraction planes, respectively, of HA (JCPDS #9-432). The apatite (002) diffraction peak became more evident and

dx.doi.org/10.1021/am300487c | ACS Appl. Mater. Interfaces 2012, 4, 3148−3156

appeared sharp after 24 h of incubation. The (211) diffraction peaks also became narrower with a longer time. In addition, other diffraction apatite peaks (200, 211, 222, and 004) also became more evident.

Mechanical Properties. The compression test results of the PCL/BG hybrids and control PCL are illustrated in Figure 8. Each of the curves is a representative for each composition.

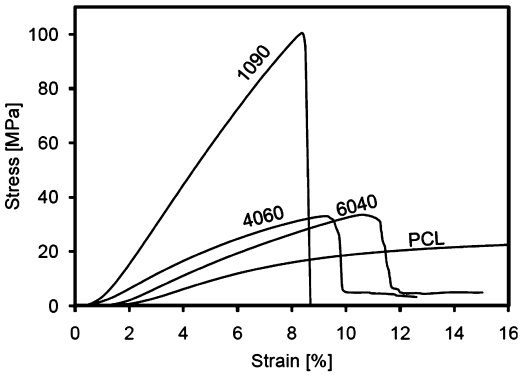

Figure 8. Representative stress–strain curves for pure PCL and different compositions of PCL/BG hybrid samples as obtained from uniaxial compressive testing.

The mean values and standard deviations of compressive modulus, compressive strength, and strain at failure of the PCL/BG hybrids and control PCL obtained from the current study are summarized in Table 2. It can be seen that the

Table 2. Summary of the Mechanical Properties of the PCL/BG Hybrids and PCL Samples (n = 5) as Obtained from the Uniaxial Compressive Testing[a]

sample ID	strain at failure [%]	compressive strength [MPa]	compressive modulus [MPa]
1090	7.67 ± 0.52 a	88.58 ± 9.57 a	1388.6 ± 75.87 a
4060	9.76 ± 0.98 b	30.89 ± 4.08 b	633.3 ± 45.38 b
6040	10.81 ± 1.53 b	28.95 ± 2.80 b	552.62 ± 30.37 b
PCL		19.79 ± 1.05 c	335 ± 11.92 c

[a]Different letters indicate that the groups are significantly different at $p < 0.05$.

incorporation of the PCL within the inorganic network significantly increased the strain at failure from 7.67 ± 0.52% for 1090 to 10.81 ± 1.53% for 6040 ($p < 0.05$). On the other hand, the presence of the inorganic component in the hybrid system also contributed to an increase in the compressive modulus and compressive strength. The four compositions shown in Table 2 were separated into three significant groups ($p < 0.05$).

Cytotoxicity Assay. The cytotoxicity of the PCL/BG hybrid samples were assessed by the MTT assay, and the results are presented in Figure 9. As can be seen, the cell viability data showed that the addition of the as-prepared PCL/BG hybrid powder suspension into the cell culture demonstrated no significant toxicity ($p > 0.05$) to the cell viability compared to the cell density after a 6 h culture on the TCPS. However, slight reductions in the optical density (OD) values were observed for the higher polymer content (6040). In addition for all compositions, an increase in OD value was observed after 24 and 72 h incubation periods, suggesting that while the growth rate may be lower than the TCPS control, cells were actively

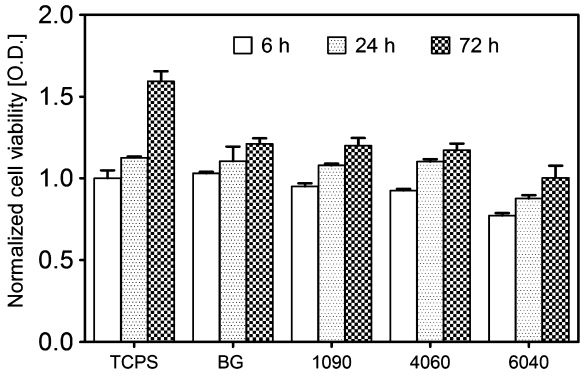

Figure 9. Normalized MC3T3-E1 cell viability after culturing in direct contact with BG, 1090, 4060, and 6040 PCL/BG hybrid particulates with concentrations of 500 μg/mL, for periods of 6, 24, and 72 h.

metabolizing on all hybrid materials for the 72 h culture period. The data in Figure 9 is for 500 μg/mL powdered hybrid materials added to the cell culture; however, the results for the 100, 200, and 300 μg/mL were consistent with Figure 9 (see Supporting Information Figure S3).

DISCUSSION

Organic–inorganic hybrid biomaterials synthesized by a sol–gel process are becoming one of the most sought-after classes of materials in scaffold fabrication for bone tissue regeneration.[13,32] More specifically, the use of biodegradable polymers such as PCL in the sol–gel process would be an interesting option, due to its biocompatibility and biodegradability. Although there are literature reports of PCL/BG glasses based on the sol–gel process,[33,34] PCL is not often added to the sol while the network is being formed during the polycondensation. Instead, sol-gel derived and sintered BGs are combined with PCL matrices. Unlike the present work, however, these nanocomposites are not considered to be hybrid materials whereby the bioactive glass components and the polymer chains are interacting via chemical bonding on a molecular scale forming a single phase. The most relevant work to the current study was conducted by Rhee and co-workers[22,35,36] who reported sol–gel derived PCL/silica materials where the PCL was added during the silicate hydrolysis stage. Sol–gel chemistry is inherently carried out with water as the main solvent for hydrolysis of the silicate component. This, in turn, means that the organic polymer must have a high molecular weight and be water soluble. Unfortunately, these criteria are met only by nonbiodegradable polymers such as polyvinyl alcohol (PVA) or polyvinyl pyrrolidone (PVP). If the polymer is degradable and water soluble but has low molecular weight, it will be leached out or segregated easily. Because high molecular weight PCL tends to precipitate in the presence of water during the sol–gel process (owing to its water insolubility), Rhee et al.[35] used a low molecular weight (2000 g/mol) water soluble and degradable α,ω-hydroxyl PCL. In order to overcome leaching and segregation of this low molecular weight α,ω-hydroxyl PCL, it was chemically linked to 3-isocyanatopropyl triethoxysilane which was then co-condensed with TEOS. Contrary to these cited works, the present study did not require the use of a coupling agent since we have utilized a high molecular weight PCL (80 000 g/mol) that does not leach out from the hybrid. Since high molecular weight PCL was not water soluble, we addressed this challenge using MEK as a cosolvent to ensure

that we had a homogeneous system at all times during the polycondensation.[12]

Previously, we reported the synthesis and characterization of novel organic−inorganic hybrid materials based on PCL and tertiary BG with uniformly distributed calcium for potential applications in bone tissue engineering.[12] However, the effects of composition on properties such as the bioactivity, mechanical properties, and biocompatibility of these materials were not investigated. In the present study, we hypothesized that the presence of surface silanol groups (Si−OH) and the incorporation of both calcium and phosphate ions into the hybrid system accelerates the in vitro bioactivity behavior. To test this hypothesis, three different PCL/BG hybrids with different composition were prepared with anticipated bioactivity and enhanced mechanical properties as compared to studies conducted by different groups, which used either nondegradable polymers[15,16,37] or silica as the only inorganic phase in the hybrid system.[15,22,38] The reason for restricting the maximum PCL content in the hybrid system to 60 wt % (i.e., 6040) was due to the fact that the hydrophobic nature of PCL limited its solubility in the inorganic sol even with MEK cosolvent . Our data (Figure 1) demonstrated that all the PCL/BG hybrids, except for the pure PCL, showed a bone-like apatite forming ability in SBF. The FTIR spectra (Figure 6) revealed that HA formation was higher with increased inorganic content (1090 and 4060) than lower inorganic content (6040). This result, while consistent with a literature report,[22] is significant due to the use of the tertiary BG as the inorganic phase and the biodegradable polymer (PCL) as an organic phase, combinations that are not reported to date. Perhaps, the most striking finding of our study is the fact that we were able to observe a well-structured HA layer formation at a very low incubation time of 6 h regardless of the PCL-BG composition. In PCL/silica sol−gel materials incorporating calcium, previous studies[22,39] have demonstrated the need for 7 days of incubation in SBF to obtain meaningful HA layers. Furthermore, an attempt to induce rapid HA deposition by annealing the samples at elevated temperature (200 °C) had a detrimental effect.[40] Careful examination of these cited studies indicate that phosphate groups were notably absent in the sol−gel hybrid materials. Given that HA deposition study in the present work was done on hybrid samples containing tertiary glass components, we believe that the phosphate was responsible for rapid HA deposition rather than the PCL-BG composition. For all compositions and incubation times, the deposited HA morphology was not different but the deposited film thickness increased significantly over time (Figure 4).

Since the growth of the apatite layer is known to be affected by the presence of PO_4^{3-} and Ca^{2+} ions,[41,42] the amounts of the Ca^{2+} and PO_4^{3-} ions present in the inorganic phase of the present hybrid system were initially optimized on the basis of the condition where a greater bioactivity is observed as reported in other studies.[43] The bioactivity data on different PCL/BG ratios used in the current study indicated that the amount of Ca and P ions in the hybrid materials influenced the HA deposition. The total amount of Ca^{2+} and PO_4^{3-} ion released from the specimens into SBF and subsequently consumed (Figures 5 and S2, Supporting Information) to form the apatite layer on the PCL/BG hybrid surfaces were directly proportional to the amount of the inorganic content incorporated in the hybrid system. In addition to the phosphate groups present in the bioactive glass, the rapid apatite nucleation observed in our system (6 h) could also be related to the presence of high concentration silanol groups on the PCL/BG surfaces and the increased overall ionic activity of the solution.[44] Once the apatite nuclei are formed, the layer can grow spontaneously by consuming the Ca^{2+} and PO_4^{3-} ions from SBF; this is because the SBF is supersaturated with respect to the apatite.

The choice of PCL in this study was to provide biodegradability and to optimize the mechanical properties of the hybrid systems. It has been reported[22,35] that low molecular weight PCL accelerates the biodegradability of PCL/silica hybrids and affects the mechanical properties whereby higher PCL contents resulted in polymer-like ductile−tough fracture behavior.[22] Conversely, the low PCL content in the hybrid led to a ceramic-like hard−brittle fracture behavior. With respect to the fracture failure, our data is consistent with the above notion. In the present study, the compressive stress and modulus values increased with the increase in BG content and vice versa (Figure 8, Table 2). Maximum compressive strength and modulus values of 90 MPa and 1.4 GPa, respectively, were achieved for 90% BG content. When we compared our data with the closest study in the literature,[22] there was a notable difference since, contrary to the cited work, both the compressive strength and modulus of our PCL/BG hybrid system significantly increased with the increase in the BG content. Given the PCL molecular weight difference between these studies and the experimental conditions involved, direct comparison is somewhat difficult. However, our data underscores the predictability of the mechanical properties of the current PCL/BG hybrids, collectively suggesting that, by combining a tertiary BG and a biodegradable PCL polymer, the mechanical properties and HA formation could be modulated.

In addition to the bioactivity and mechanical properties, biomaterials used for bone regeneration also need to be cytocompatible, without eliciting adverse response from the application site or surrounding tissue. Various studies[24−28,33,34] demonstrated that polymer/BG hybrid materials synthesized by a sol−gel process and have undergone a thermal stabilization at high temperature (ca. 600 °C) to be nontoxic since the high temperature burns off residual and leachable toxic components including the polymer. However, the PCL/BG hybrids derived from the sol−gel process in this study could not be thermally treated at high temperature, since it would lead to degradation of the PCL. In view of this, the effect of the possible unreacted precursors on cell viability was evaluated. As shown in Figure 9, the result from the cytotoxicity assay of PCL/BG hybrids indicated that the present materials were not significantly toxic when compared with the TCPS control for each time point. Cell viability studies on sol−gel derived BG hybrid biomaterials were reported primarily for PVA systems.[8,29,45] It seems that the cytocompatibility in the PVA hybrid systems is dependent on cell type. For example, when primary cells are cultured on these materials, cell viability is generally poor[29] whereas stem cells (both bone marrow and adipose-derived) showed excellent viability.[8,45] Although we did not utilize stem cells in this study, the osteoblast-like cells viability on the PCL/BG hybrid system is better than PVA/BG hybrids on primary cell viability whereas it is comparable to the stem cell data.

Taken together, the PCL/BG hybrids synthesized via a sol−gel process demonstrated some of the advantages of combining biodegradable polymers with tertiary BGs. The ability to use a single material, polymer or glasses, for such purposes may be impractical, and hybrids may be utilized to yield better results. Such is the case with organic−inorganic hybrids, which can

exhibit a range of bioactive, resorbable, and mechanical properties. Further tailoring of the material chemistry and morphology can thus be employed to match these properties with the host tissue, in an effort to give better incorporation and enhanced efficacy.

CONCLUSION

In this study, in vitro bone-like HA formation ability, mechanical properties, and biocompatibility of sol−gel derived PCL/BG hybrids based on tertiary glasses were investigated. It was shown that the bioactivity of sol−gel derived BG is mainly governed by the presence of surface silanol group (Si−OH) and Ca and P content. After incubating in SBF, all hybrid materials showed HA formation ability. However, the rate and total amount of HA formation decreased with an increase in PCL content (Figure 5). The strain at fracture increased with an increase in PCL content whereas the compressive modulus and strength of the PCL/BG hybrids increased with the decrease in PCL content. The cytotoxicity test indicated that no significant ($p > 0.05$) toxicity was observed for lower polymer contents; however, a slight reduction in cell viability was observed with the higher polymer content as compared to the control. Therefore, the ability to tailor the bioactivity and mechanical property of these novel PCL/BG hybrid materials could represent a potential application for bone tissue regeneration.

ASSOCIATED CONTENT

Supporting Information

Ionic compositions (mM) of SBF and human blood plasma; high magnification SEM micrographs and the corresponding EDX patterns for the evolution of the HA layer on 6040 PCL/BG hybrid disks before and after incubation in SBF for different time points; Ca^{2+}, PO_4^{3-}, and Si ion concentration in SBF as a function of soaking time for PCL and PCL/BG hybrids with different compositions; normalized MC3T3-E1 cells viability after culturing in direct contact with different concentrations of BG, 1090, 4060, and 6040 for different time points. This material is available free of charge via the Internet at http://pubs.acs.org

AUTHOR INFORMATION

Corresponding Author

*E-mail: kmequani@uwo.ca (K.M.); arizkalla@eng.uwo.ca (A.S.R.). Tel: +1 (519) 661-2111 ext. 88573 (K.M.) or 86086 (A.S.R.). Fax: + 1(519) 661-3498.

Notes

The authors declare no competing financial interest.

ACKNOWLEDGMENTS

The authors acknowledge the financial support by the Natural Science and Engineering Research Council (NSERC) of Canada and the CIHR Joint Motion Training Program in Musculoskeletal Health Research (JUMP) and Prof. Jeff Dixon and Ms. Elizabeth Pruski for their valuable technical assistance.

REFERENCES

(1) Arcos, D.; Vallet-Regi, M. *Acta Biomater.* **2010**, *6*, 2874−2888.
(2) Puppi, D.; Chiellini, F.; Piras, A. M.; Chiellini, E. *Prog. Polym. Sci.* **2010**, *35*, 403−440.
(3) Khan, Y.; Yaszemski, M. J.; Mikos, A. G.; Laurencin, C. T. *J. Bone Joint Surg. Am.* **2008**, *90* (Suppl1), 36−42.
(4) Martin, R. A.; Yue, S.; Hanna, J. V.; Lee, P. D.; Newport, R. J.; Smith, M. E.; Jones, J. R. *Philos. Trans. R. Soc., A: Math., Phys. Eng. Sci.* **2012**, *370*, 1422−1443.
(5) Stevens, B.; Yang, Y.; Mohandas, A.; Stucker, B.; Nguyen, K. T. *J Biomed. Mater. Res. B Appl. Biomater.* **2008**, *85*, 573−572.
(6) Stevens, M. M. *Mater.Today* **2008**, *11*, 18−25.
(7) Jell, G.; Notingher, I.; Tsigkou, O.; Notingher, P.; Polak, J. M.; Hench, L. L.; Stevens, M. M. *J. Biomed. Mater. Res., Part A* **2008**, *86*, 31−40.
(8) Gomide, V. S.; Zonari, A.; Ocarino, N. M.; Goes, A. M.; Serakides, R.; Pereira, M. M. *Biomed. Mater.* **2012**, *7*, 015004.
(9) Fu, Q.; Saiz, E.; Rahaman, M. N.; Tomsia, A. P. *Mater. Sci. Eng., C: Mater. Biol. Appl.* **2011**, *31*, 1245−1256.
(10) Gloria, A.; De Santis, R.; Ambrosio, L. *J. Appl. Biomater. Biomech.* **2010**, *8*, 57−67.
(11) Guan, L. M.; Davies, J. E. *J. Biomed. Mater. Res., Part A* **2004**, *71A*, 480−487.
(12) Allo, B. A.; Rizkalla, A. S.; Mequanint, K. *Langmuir* **2010**, *26*, 18340−18348.
(13) Pandey, S.; Mishra, S. B. *J. Sol-Gel Sci.Technol.* **2011**, *59*, 73−94.
(14) Valliant, E. M.; Jones, J. R. *Soft Matter* **2011**, *7*, 5083−5095.
(15) Pereira, M. M.; Jones, J. R.; Orefice, R. L.; Hench, L. L. *J. Mater. Sci. Mater. Med.* **2005**, *16*, 1045−1050.
(16) Rhee, S. H.; Hwang, M. H.; Si, H. J.; Choi, J. Y. *Biomaterials* **2003**, *24*, 901−906.
(17) Poologasundarampillai, G.; Ionescu, C.; Tsigkou, O.; Murugesan, M.; Hill, R. G.; Stevens, M. M.; Hanna, J. V.; Smith, M. E.; Jones, J. R. *J. Mater. Chem.* **2010**, *20*, 8952−8961.
(18) Rho, J. Y.; Kuhn-Spearing, L.; Zioupos, P. *Med. Eng. Phys.* **1998**, *20*, 92−102.
(19) Kokubo, T.; Kushitani, H.; Sakka, S.; Kitsugi, T.; Yamamuro, T. *J. Biomed. Mater. Res.* **1990**, *24*, 721−734.
(20) Webster, T. J.; Ergun, C.; Doremus, R. H.; Siegel, R. W.; Bizios, R. *J. Biomed. Mater. Res.* **2000**, *51*, 475−483.
(21) Jones, J. R. *J. Eur. Ceram. Soc.* **2009**, *29*, 1275−1281.
(22) Rhee, S. H. *Biomaterials* **2004**, *25*, 1167−1175.
(23) Yoo, J. J.; Lee, J. E.; Kim, H. J.; Kim, S. J.; Lim, J. H.; Lee, S. J.; Lee, J. I.; Lee, Y. K.; Lim, B. S.; Rhee, S. H. *J. Biomed. Mater. Res., Part B: Appl. Biomater.* **2007**, *83*, 189−198.
(24) Valerio, P.; Guimaraes, M. H.; Pereira, M. M.; Leite, M. F.; Goes, A. M. *J. Mater. Sci.: Mater. Med.* **2005**, *16*, 851−856.
(25) Zhang, K.; Washburn, N. R.; Simon, C. G., Jr. *Biomaterials* **2005**, *26*, 4532−4539.
(26) Yun, H. S.; Park, J. W.; Kim, S. H.; Kim, Y. J.; Jang, J. H. *Acta Biomater.* **2011**, *7*, 2651−2660.
(27) Meseguer-Olmo, L.; Ros-Nicolas, M. J.; Clavel-Sainz, M.; Vicente-Ortega, V.; Alcaraz-Banos, M.; Lax-Perez, A.; Arcos, D.; Ragel, C. V.; Vallet-Regi, M. *J. Biomed. Mater. Res.* **2002**, *61*, 458−465.
(28) Bielby, R. C.; Pryce, R. S.; Hench, L. L.; Polak, J. M. *Tissue Eng.* **2005**, *11*, 479−488.
(29) Costa, H. S.; Stancioli, E. F.; Pereira, M. M.; Orefice, R. L.; Mansur, H. S. *J. Mater. Sci. Mater. Med.* **2009**, *20*, 529−535.
(30) Rehman, I.; Knowles, J. C.; Bonfield, W. *J. Biomed. Mater. Res.* **1998**, *41*, 162−166.
(31) Landi, E.; Celotti, G.; Logroscino, G.; Tampieri, A. *J. Eur. Ceram. Soc.* **2003**, *23*, 2931−2937.
(32) Rhee, S. H. *Biomaterials* **2003**, *24*, 1721−1727.
(33) Jo, J. H.; Lee, E. J.; Shin, D. S.; Kim, H. E.; Kim, H. W.; Koh, Y. H.; Jang, J. H. *J. Biomed. Mater. Res., Part B: Appl. Biomater.* **2009**, *91*, 213−220.
(34) Lee, H. H.; Yu, H. S.; Jang, J. H.; Kim, H. W. *Acta Biomater.* **2008**, *4*, 622−629.
(35) Rhee, S. H.; Choi, J. Y.; Kim, H. M. *Biomaterials* **2002**, *23*, 4915−4921.
(36) Rhee, S. H.; Lee, Y. K.; Lim, B. S.; Yoo, J. J.; Kim, H. J. *Biomacromolecules* **2004**, *5*, 1575−1579.
(37) Pereira, M. M.; Jones, J. R.; Hench, L. L. *Adv. Appl. Ceram.* **2005**, *104*, 35−42.

(38) Eglin, D.; Ali, S. A. M.; Perry, C. C. *Polym. Int.* **2003**, *52*, 1807−1819.
(39) Rhee, S. H. *J. Biomed. Mater. Res.* **2003**, *67A*, 1131−1138.
(40) Yoo, J. J.; Rhee, S. H. *J. Biomed. Mater. Res.* **2004**, *68*, 401−410.
(41) Padilla, S.; Roman, J.; Carenas, A.; Vallet-Regi, M. *Biomaterials* **2005**, *26*, 475−483.
(42) Li, R.; Clark, A. E.; Hench, L. L. *J. Appl. Biomater.* **1991**, *2*, 231−239.
(43) Salinas, A. J.; Martin, A. I.; Vallet-Regi, M. *J. Biomed. Mater. Res.* **2002**, *61*, 524−532.
(44) Yan, X.; Huang, X.; Yu, C.; Deng, H.; Wang, Y.; Zhang, Z.; Qiao, S.; Lu, G.; Zhao, D. *Biomaterials* **2006**, *27*, 3396−3403.
(45) Gomide, V.; Zonari, A.; Breyner, N.; de Goes, A.; Pereira, M. *ISRN Mater. Sci.* **2011**, 240864.